

Vanadium in silicon: Lattice positions and electronic properties

Jack Mullins, Vladimir P. Markevich, Matthew P. Halsall, and Anthony R. Peaker

Photon Science Institute and School of Electrical and Electronic Engineering, University of Manchester, Manchester M13 9PL, United Kingdom

(Received 23 January 2017; accepted 20 March 2017; published online 4 April 2017)

The electronic properties of vanadium in silicon have been studied using deep level transient spectroscopy (DLTS), high resolution Laplace DLTS, capacitance voltage measurements and secondary ion mass spectroscopy (SIMS). Vanadium was implanted into float zone (FZ) grown n-type and FZ and Czochralski (Cz) grown p-type Si and implantation damage was removed through annealing between 700 and 900 °C. DLTS measurements were carried out to determine the electronic characteristics of vanadium-related defects in silicon. It is argued that the dominant electrically active defect is related to interstitial vanadium (V_i) atoms. The distribution of implanted vanadium is seen to differ between Czochralski and FZ silicon, with redistribution of vanadium atoms occurring significantly faster in Cz-Si. We suggest that in FZ-Si the V_i atoms interact with implantation induced vacancies and move to the substitutional site where they are much less mobile. At the peak concentration of vanadium, determined by SIMS to be $\sim 10^{15} \text{ cm}^{-3}$ in FZ-Si, the electrically active fraction is significantly lower ($\sim 10^{13} \text{ cm}^{-3}$). As we see no evidence of precipitation occurring in the region close to the implant peak, it is concluded that a large portion of V atoms should be located at the substitutional site. Despite the *ab-initio* modeling predictions of substitutional vanadium, V_s , introducing a shallow acceptor level in the silicon band gap, no electrical activity associated with the V_s fraction has been observed in this work in spite of its concentration being at a measurable level. As such, our results indicate that substitutional vanadium is electrically inactive in silicon. © 2017 Author(s). All article content, except where otherwise noted, is licensed under a Creative Commons Attribution (CC BY) license (<http://creativecommons.org/licenses/by/4.0/>). [<http://dx.doi.org/10.1063/1.4979697>]

Transition metal impurities are known to introduce deep level states in the silicon band gap that can act as strong recombination centers, severely affecting the performance of electronic and photovoltaic devices.¹ The scale of this effect depends on both the concentration of the metal contaminant and the levels it introduces, with deep levels acting as particularly harmful Shockley Read Hall recombination centers with severe effects on minority carrier lifetime. Although the concentration of transition metal impurities is low in electronic grade silicon fabricated through the Czochralski (Cz) or float zone (FZ) growth processes, it can be orders of magnitude higher in materials that have not undergone a Siemens-like purifying process.² As such, understanding the behavior of transition metals in silicon is necessary to reduce their effects in areas where the purifying processes are not economically feasible, for example, in low cost polycrystalline silicon feedstock for the solar photovoltaic industry.³ This feedstock is used in the production of block cast multicrystalline silicon and upgraded metallurgical grade silicon for solar cells.

One transition metal known to have a particularly large effect on solar cell performance is vanadium, which has been shown to reduce cell efficiency at concentrations as low as 10^{12} cm^{-3} .⁴ The minimum energy position of vanadium in silicon is thought to be interstitial, but its diffusion coefficient is around 1000 times lower than that for interstitial iron at 1000 °C.⁵ This makes vanadium very difficult to getter,⁶ and hence it can remain in silicon as a powerful lifetime killer.

Previous studies have shown that interstitial vanadium (V_i), observed in electron paramagnetic resonance (EPR) measurements to occupy the tetrahedral interstitial site,^{7,8} presents 3 deep level states in the silicon band gap.^{1,4,9–11} These states are thought to correspond to the first acceptor level $V_i^{-/0}$ ($E_c - 0.20 \text{ eV}$), the first donor level $V_i^{0/+}$ ($E_c - 0.45 \text{ eV}$) and the second donor level $V_i^{+/++}$ ($E_v + 0.34 \text{ eV}$) of interstitial vanadium; however, some disagreement is seen in the literature on the nature of the level at $E_c - 0.20 \text{ eV}$, with photoionisation cross section measurements suggesting that it is donor-like rather than acceptor-like in nature.¹⁰ However, the value of directly measured capture cross section of electrons indicates it is an acceptor.⁹ A summary of the data on the previously observed electrically active levels attributed to interstitial vanadium across a range of studies is given in Table I.

A number of studies employing density functional theory (DFT) to study vanadium in Si have been carried out, which in general predict the electrically active levels close to those observed experimentally.^{12–15} The most recent DFT

TABLE I. Positions of the three energy levels (in eV) assigned to interstitial vanadium in silicon. Numbers shown in parenthesis indicate a measured barrier for capture of holes in eV.

Label	Reference 4	Reference 9	Reference 1	Reference 10	Reference 11
E_1	$E_c - 0.22$	$E_c - 0.20$	$E_c - 0.16$	$E_c - 0.21$	$E_c - 0.20$
E_2	$E_c - 0.46$	$E_c - 0.45$	$E_c - 0.45$	$E_c - 0.48$	$E_c - 0.43$
H_1	$E_v + 0.42$	$E_v + 0.34$ (0.12)	$E_v + 0.30$	$E_v + 0.36$	$E_v + 0.34$ (0.12)

studies^{12,13} of vanadium in Si suggest that interstitial vanadium lies at or close to the tetrahedral interstitial site and displays the second double donor level at $E_v + 0.40$ eV, the first donor level at $E_c - 0.52$ eV and an acceptor level at $E_c - 0.20$ eV. These values are in good agreement with the experimental results shown in Table I. Substitutional vanadium, V_s , is predicted to occur when the available silicon vacancies interact with the V_i atoms, and the V_s atoms are suggested to introduce one relatively shallow acceptor level in the silicon band gap at $E_c - 0.94$ eV ($E_v + 0.23$ eV).¹²

In this work, we have used secondary ion mass spectrometry (SIMS), deep level transient spectroscopy (DLTS) and Laplace DLTS (LDLTS) to characterize vanadium in Czochralski and float zone grown silicon.

Samples of n- and p-type float zone and p-type Czochralski silicon wafers with resistivity in the range 1–5 Ω cm were implanted with $2.0 \times 10^{11} \text{ cm}^{-2}$ vanadium ions with energy 2 MeV (n-type) and $2.6 \times 10^{11} \text{ cm}^{-2}$ vanadium ions with energy 1.3 MeV (p-type). The predicted peak concentration of vanadium in these samples was $4.8 \times 10^{15} \text{ cm}^{-3}$ (n-type) and $5.7 \times 10^{15} \text{ cm}^{-3}$ (p-type). Strips of silicon were cut from these wafers, and RCA cleaned (in 5:1:1 $\text{H}_2\text{O}:\text{H}_2\text{O}_2:\text{NH}_3$ followed by 6:1:1 $\text{H}_2\text{O}:\text{H}_2\text{O}_2:\text{HCl}$ at 70 °C) and annealed at temperatures between 700 and 900 °C in a nitrogen gas ambient for 30 min in order to remove implantation damage.

Following cleaning and heat treatment, SIMS measurements were carried out on a range of samples, while others were prepared for electrical measurement (DLTS, LDLTS and CV-IV characterization). Schottky barrier diodes (SBDs) of diameter 1 mm were formed on the surface of the silicon by evaporation of Au (n-type) through a shadow mask and through plasma sputtering of Ti and Al (p-type). Ohmic contacts were then created on the back surface through thermal evaporation of Al (n-type) or Au (p-type).

The quality of the diodes was tested using current- and capacitance-voltage measurements, which also provided the concentration of uncompensated shallow donors and acceptors, N_d . The highest quality diodes were then studied using DLTS and LDLTS measurements in order to characterize defects with deep levels. Following the conventional DLTS measurements, a number of p-type samples were studied following reverse bias annealing (RBA). In this process, the samples were annealed at 100 °C under a reverse bias of +7 V, redistributing hydrogen within the sample and allowing a region closer to the sample surface to be measured using DLTS.

Figure 1 shows the conventional DLTS spectra of n-type float zone and p-type float zone and Czochralski Si annealed at 800 °C for 30 min. In n-type silicon, two clear peaks are observed at 115 and 205 K, labelled as E_1 and E_2 in Figure 1. In both p-type Czochralski and float zone silicon, one dominant peak is observed at 260 K, labelled as H_1 . For each of these three signals, activation energies and pre-exponential factors (A) were determined from the Arrhenius plots of T^2 -corrected emission rates, which are displayed in Table II. The measured activation energies are in good agreement with the previous studies of vanadium in silicon.^{1,4,9–11,16}

Through a comparison of the measured energies with those in the literature, we have assigned the two peaks in n-type Si to the first acceptor level and first donor level of

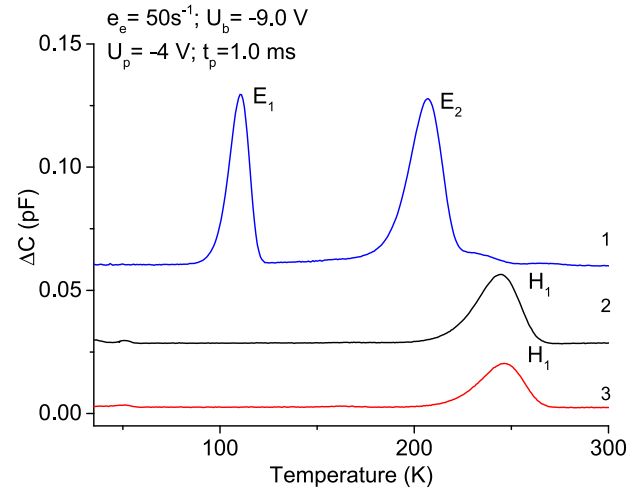


FIG. 1. DLTS spectra recorded on vanadium implanted float zone n-Si (curve 1), float zone p-Si (curve 2) and Czochralski p-Si (curve 3) annealed at 800 °C for 30 min. Spectra are shifted on the vertical axis for clarity.

interstitial vanadium and the level in p-type Si to the double donor level $V_i^{+/++}$.

The apparent capture cross sections of majority carriers, σ_{app} , for these defects have been calculated from their pre-exponential factors. The true values of capture cross sections, σ_d , of majority carriers for these defects have also been determined using Laplace DLTS measurements with varying filling pulse widths between 40 ns and 20 ms. The magnitude of the LDLTS signal for the level E_1 in n-type Si and for the level H_1 in p-type Si were both found to be variable with changing of pulse length, while for the level E_2 no changes have been observed in the n-type Si studied. This indicates a large value of capture cross sections for the E_2 level, which we could not measure with our equipment.

Figure 2 shows a comparison between the metallurgical concentrations of vanadium measured by SIMS (Figure 2(a)) with the concentration of the electrically active V_i atoms determined from DLTS measurements (Figure 2(b)) on the samples of float zone and Czochralski silicon annealed at 800 °C for 30 min. Also shown is the measured concentration of shallow donors and acceptors within the samples (Figure 2(c)).

Crucially, we observe a large difference in the changes in SIMS spectra between Czochralski and float zone silicon as a result of annealing, with the vanadium implant peak disappearing in Cz-Si at a significantly lower temperature than in FZ-Si. It is evident from the data presented in Figs. 2(a) and 3 that the diffusivity of vanadium is much higher in Cz-Si than FZ-Si.

TABLE II. Properties of the electrically active states of interstitial vanadium in silicon.

Level	ΔE (eV)	A ($\text{s}^{-1} \text{ K}^{-1}$)	σ_{app} (cm^2)	σ_d (cm^2)
E_1	$E_c - 0.20$	4.65×10^6	2.1×10^{-16}	4.3×10^{-17}
E_2	$E_c - 0.43$	5.24×10^7	1.5×10^{-15}	N/A
H_1	$E_v + 0.34$ (0.12)	3.27×10^6	4.5×10^{-17}	From 1.2×10^{-19} to 1.8×10^{-19} (255–275 K)

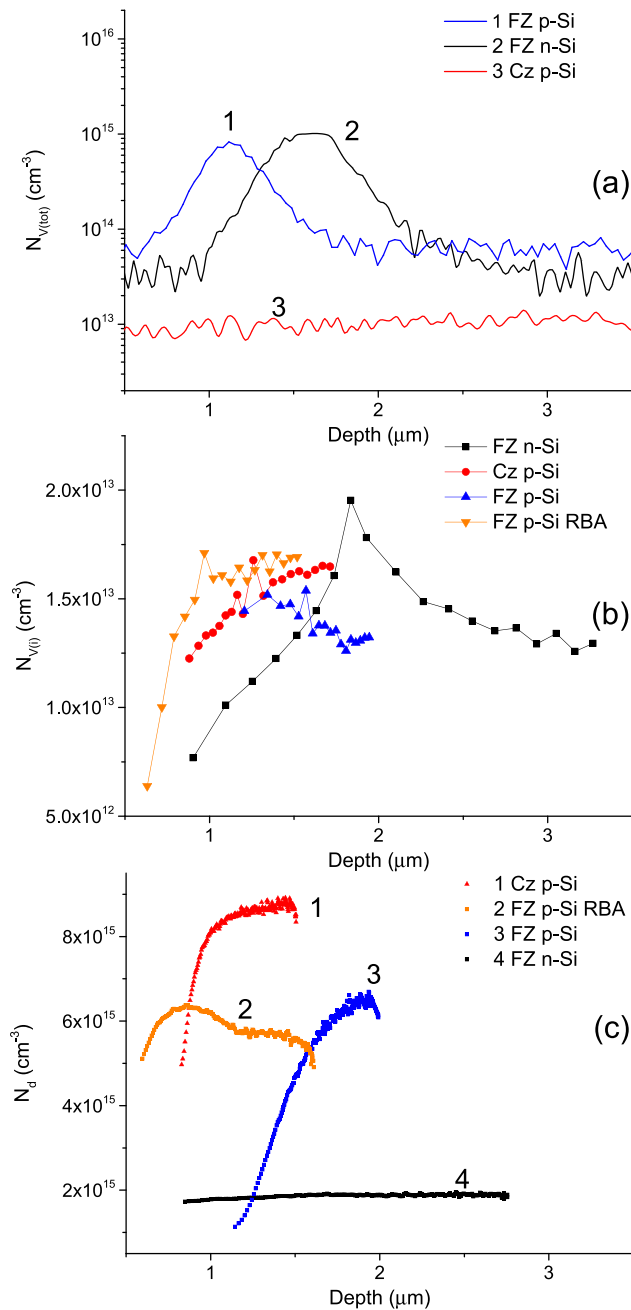


FIG. 2. Comparison of metallurgical vanadium concentration after annealing at 800 °C for 30 min measured by SIMS (a), with concentration of interstitial vanadium measured with Laplace DLTS (b) and carrier concentration determined from C-V profiling (c). Samples that have undergone reverse bias annealing are denoted RBA.

This difference in the vanadium diffusivity and distribution upon annealing is interpreted as the vanadium interstitial interacting with the implantation induced vacancies and moving to the substitutional site in the float zone case. The recent ab-initio calculations¹² indicate that isolated V in Si although preferring to remain interstitial is likely to react with vacancies at the anneal temperature (where the silicon is near intrinsic ($>650^{\circ}\text{C}$) and vacancies are in the neutral charge state) if these are pre-existing due, for example, to implantation or irradiation. In that case, V_i readily becomes V_s with a gain in energy.

In Czochralski silicon, a large proportion of vacancies are paired with oxygen, which is known to be an effective

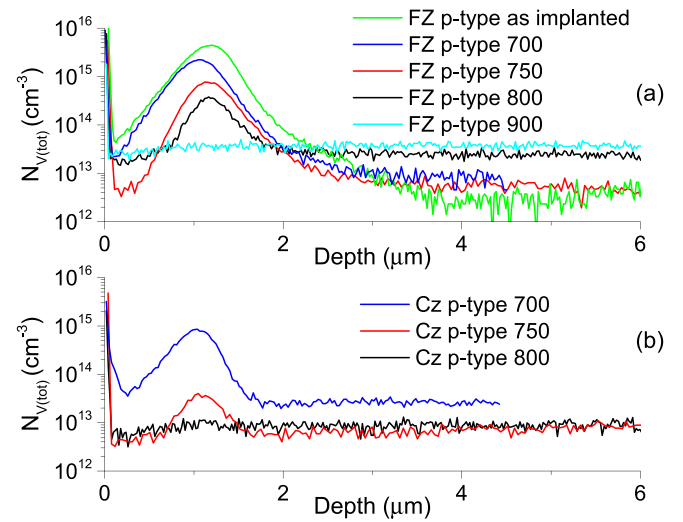


FIG. 3. Schematic representation of changes in SIMS spectra of metallurgical vanadium concentration of implanted float zone (a) and Czochralski (b) Si annealed for 30 min at a range of temperatures.

trap for vacancies and is present at typical concentrations of $\sim 10^{18}\text{cm}^{-3}$. As this oxygen concentration exceeds that of vanadium in the Cz-Si samples studied in this work, and taking into account the high thermal stability of some vacancy-oxygen complexes,¹⁷ it is suggested that the majority of the vanadium atoms will be at the interstitial site in this material.

In float zone Si, oxygen concentrations are substantially lower, resulting in greater concentrations of mobile vacancies. These vacancies can interact with interstitial vanadium atoms, leading to the formation of substitutional vanadium. Substitutional vanadium atoms are expected to be significantly less mobile than interstitial vanadium, and as such the redistribution of vanadium upon annealing can be expected to be much slower in float zone silicon.

This is observed in Figure 3, which shows the evolution of vanadium concentration profiles measured with SIMS upon annealing of both Czochralski and float zone silicon at increasing temperatures, in which the peak concentration of vanadium is seen to reduce upon higher temperature annealing. The difference in diffusivity in these materials is seen as the disappearance of the vanadium related SIMS peak measured in Czochralski material upon annealing at 800 °C, consistent with the diffusion length of interstitial vanadium observed in Ref. 5, suggesting the majority of the vanadium is in the more mobile interstitial state. In the float zone material, a peak is still observed close to the projected implantation depth after annealing at 800 °C, which eventually disappears upon annealing at 900 °C, while a small concentration of interstitial vanadium is consistently observed in DLTS.

Comparing Figures 2(a) and 2(b), we observe a large difference between the concentration of the electrically active fraction ($N_{V(i)}$) and the total metallurgical concentration ($N_{V(tot)}$) of vanadium determined by SIMS, when the metallurgical concentration is high. At peak concentration ($\sim 10^{15}\text{cm}^{-3}$), only around 3% of the vanadium is electrically active at the interstitial site. At lower metallurgical concentrations, about 30% of the vanadium is seen to be electrically active. This is similar to the values observed in

the Westinghouse study,⁴ using Cz-Si doped during growth, in which the ratio of electrically active to metallurgical vanadium concentration was seen to be 0.28.

In the case of the Cz p-type Si after the 800 °C anneal, the metallurgical concentration determined by SIMS is relatively uniform throughout the measured depth. In this case, the value of the vanadium concentration determined from SIMS measurement is close to the detection limit, and within the combined errors of SIMS and DLTS, the metallurgical concentration is approximately equal to the concentration of the electrically active interstitial vanadium atoms.

The decrease in peak concentration upon annealing indicates that the vanadium is diffusing away from the implant peak and not agglomerating into precipitates at the projected depth. In the cases of the transition metals late in the 3d series with much higher diffusion coefficients (e.g., Fe and Ni), precipitates are formed nucleating randomly or at extended defects. The SIMS profiles of implants of these metals show a very characteristic behaviour due to the Ostwald ripening of the precipitates. Such SIMS profiles show a characteristic narrowing, and the precipitates can often be seen in transmission electron microscopy (TEM). These precipitates have distinct electrical characteristics easily identifiable in DLTS by their line shapes and unusual carrier capture behaviour.^{18,19}

In contrast, the slow diffusing early transition metals of the 3d series (e.g., Ti) do not form large precipitates although “nano-precipitates” have been detected by DLTS. These are almost impossible to detect by TEM, as they tend to be very small (~5 nm) and at low metal concentrations do not have a high areal density.^{20,21}

However, they are easily detected by DLTS and, as in the case of larger precipitates, have a very distinctive but different carrier capture behaviour compared to the larger metal particles. The DLTS signal from nano-precipitates appears to be independent of the metal species but dependent on the size to a small degree, but quite distinctive and so easily identifiable.²⁰ In the heat-treated vanadium-implanted samples, we see no DLTS signals characteristic of the larger precipitates but in some p-type samples DLTS evidence of nano-precipitates has been found. The key issue that we need to consider is whether the difference in chemical concentration (from SIMS) and concentration of V_i (from DLTS) is due to the migration of V_i to substitutional sites or to nano-precipitates. We see a DLTS signal characteristic of nano-precipitates only in the near surface region (<0.6 μm from the surface) of some heat-treated p-type Si samples. There is no nano-precipitate related signal near the physical location of the implant peak. The near surface nano-precipitates are prominent in the Cz material annealed in the temperature range 800–900 °C but are also evident in the 900 °C annealed FZ samples. The results of the DLTS study of vanadium related nano-precipitates will be published in more detail elsewhere. If we examine the SIMS measurements on these samples, we see no evidence of a significant increase in the concentration of vanadium corresponding to the location of the nano-precipitates, so we can say, with confidence that the nano-precipitates constitute less than 1% of the vanadium atoms observed by SIMS in the vicinity of the implant peak.

This evidence, combined with the low diffusivity of vanadium in the case of FZ samples, is a strong indication that the majority of vanadium close to the implant peak is located at the substitutional site. However, it has been predicted by the first principles calculations that substitutional vanadium should have an acceptor level at $E_v + 0.23 \text{ eV}$.¹² If this is the case, it should be easily detectable in DLTS in p-type and by MCTS in n-type. We do not detect such a level.

If substitutional vanadium possesses a shallow acceptor level, it should cause a dip in the free carrier concentration profiles in n-type and a peak in p-type Si at the projected depth. From the difference in the $N_{V(\text{tot})}$ and $N_{V(i)}$ concentrations measured by SIMS and DLTS, the expected concentration of V_s and hence the change in free carrier concentration would be $\sim 10^{15} \text{ cm}^{-3}$. Measurements of the free carrier concentration have been performed at a range of temperatures, and no such effect has been observed as can be seen in Figure 2(c). The carrier concentration profiles determined from C-V measurements shown in Figure 2(c), combined with the lack of observed peaks due to V_s in the DLTS spectra shown in Figure 1, indicate that the substitutional vanadium is likely to be electrically inactive.

The lack of detection of the theoretically predicted acceptor level of V_s could be explained due to the inherent inaccuracy of the energy level calculations. Calculations of the energy level positions are difficult from first principles needing adjustments to correct the calculated band gap using a marker method. It is possible that within the possible calculation errors, the level of V_s rather than being a shallow acceptor lies in the band and hence would not be detectable using DLTS, or carrier concentration measurements. Some support for this idea is given by the fact that no one has ever detected an electrical level of V_s experimentally.

We have shown that interstitial vanadium presents three levels in the silicon band gap at $E_c - 0.20 \text{ eV}$, $E_c - 0.43 \text{ eV}$ and $E_v + 0.34 \text{ eV}$, in good agreement with the corresponding values in the literature. The direct majority capture cross section values have been determined for two of these levels, E_1 and H_1 to be 4.3×10^{-17} and $3.5 \times 10^{-17} \exp[-0.12(\text{eV})/kT] \text{ cm}^2$, respectively.

We see that the redistribution of vanadium is different in float zone and Czochralski grown material, with diffusion occurring much faster in Czochralski Si, and argue this is due to the significant fraction of less mobile substitutional V atoms in the FZ-Si. Finally, we see no indication of electrical activity due to substitutional vanadium and argue that it is likely to be electrically inactive.

This work has been supported by the EPSRC under the Supergen Contract No. EP/M024911/1. We would like to thank José Coutinho and Paulo Santos at the University of Aveiro for the detailed discussions regarding this work. The SIMS measurements were undertaken by Dr. Alison Chew of Loughborough Surface Analysis Ltd.

¹E. R. Weber, *Appl. Phys. A* **30**, 1 (1983).

²S. Pizzini, *Sol. Energy Mater. Sol. Cells* **94**, 1528 (2010).

³A. R. Peaker, V. P. Markevich, B. Hamilton, G. Parada, A. Dudas, A. Pap, E. Don, B. Lim, J. Schmidt, L. Yu, Y. Yoon, and G. Rozgonyi, *Phys. Status Solidi A* **209**, 1884 (2012).

- ⁴J. R. Davis, A. Rohatgi, R. H. Hopkins, P. D. Blais, P. Rai-Choudhury, J. R. McCormick, and H. C. Mollenkopf, *IEEE Trans. Electron Devices* **27**, 677 (1980).
- ⁵T. Sadoh and H. Nakashima, *Appl. Phys. Lett.* **58**, 1653 (1991).
- ⁶R. Singh, S. J. Fonash, and A. Rohatgi, *Appl. Phys. Lett.* **49**, 800 (1986).
- ⁷H. H. Woodbury and G. W. Ludwig, *Phys. Rev.* **117**, 102 (1960).
- ⁸J. J. van Kooten, D. van Kootwijk, and C. A. J. Ammerlaan, *J. Phys. C* **20**, 841 (1987).
- ⁹T. Sadoh, H. Nakashima, and T. Tsurushima, *J. Appl. Phys.* **72**, 520 (1992).
- ¹⁰L. Tilly, H. G. Grimmeiss, H. Pettersson, K. Schmalz, K. Tittelbach, and H. Kerkow, *Phys. Rev. B* **44**, 12809 (1991).
- ¹¹J. Mullins, V. P. Markevich, M. P. Halsall, and A. R. Peaker, *Phys. Status Solidi A* **213**, 2838 (2016).
- ¹²D. J. Backlund, T. M. Gibbons, and S. K. Estreicher, *Phys. Rev. B* **94**, 195210 (2016).
- ¹³A. G. Marinopoulos, P. Santos, and J. Coutinho, *Phys. Rev. B* **92**, 075124 (2015).
- ¹⁴F. Beeler, O. K. Andersen, and M. Scheffler, *Phys. Rev. Lett.* **55**, 1498 (1985).
- ¹⁵H. Katayama-Yoshida and A. Zunger, *Phys. Rev. B* **31**, 8317 (1985).
- ¹⁶R. Pässler, H. Pettersson, H. G. Grimmeiss, and K. Schmalz, *Phys. Rev. B* **55**, 4312 (1997).
- ¹⁷L. I. Murin, J. L. Lindström, V. P. Markevich, A. Misiuk, and C. A. Londos, *J. Phys.: Condens. Matter* **17**, S2237 (2005).
- ¹⁸M. Seibt, H. Hedemann, A. A. Istratov, F. Riedel, A. Sattler, and W. Schröter, *Phys. Status Solidi A* **171**, 301 (1999).
- ¹⁹A. R. Peaker, B. Hamilton, G. R. Lahiji, I. E. Ture, and G. Lorimer, *Mater. Sci. Eng. B* **4**, 123 (1989).
- ²⁰S. Leonard, V. P. Markevich, A. R. Peaker, B. Hamilton, K. Yousseff, and G. Rozgonyi, *Phys. Status Solidi B* **251**, 2201 (2014).
- ²¹M. Polignano, C. Bresolin, G. Pavia, V. Soncini, F. Zanderigo, G. Queirolo, and M. Di Dio, *Mater. Sci. Eng. B* **53**, 300 (1998).